Characterization of neutrophil function in Papillon-Lefèvre syndrome

Roberts, Helen; White, Phillipa; Dias, Irundika H. K.; McKaig, Sarah; Veeramachaneni, Ratna; Thakker, Nalin; Grant, Melissa; Chapple, Iain

DOI:
10.1189/jlb.5A1015-489R

Characterisation of neutrophil function in Papillon-Lefèvre Syndrome

Summary sentence

Neutrophils from Papillon-Lefèvre Syndrome (PLS) patients exhibit multiple functional abnormalities (ROS, NETs, Chemotaxis and cytokine release), which together may explain pre-pubertal periodontitis in PLS (24 words).

Running title

Neutrophil function in Papillon-Lefèvre Syndrome.

Authorship

Helen Roberts[1+], Phillipa White[1+], Irundika Dias[2], Sarah McKaig[3], Ratna Veeramachaneni[4] Nalin Thakker[4] Melissa Grant[1+] and Iain Chapple[1+]*.

*Corresponding author: I.L.Chapple@bham.ac.uk, +44 (0)121 466 5486 (Secretary)

[+]These authors contributed equally

Addresses

1. Periodontal Research Group and MRC-Centre for Immune Regulation, School of Dentistry, University of Birmingham, St Chads Queensway, Birmingham, B4 6NN

2. Aston Research Centre for Healthy Ageing, School of Life and Health Sciences, Aston University, Aston Triangle, Birmingham, B4 7ET

3. Department of Dental Specialties Birmingham Children's Hospital NHS Foundation Trust, Steelhouse Lane, Birmingham, B4 6NH

4. School of Dentistry, The University of Manchester, Higher Cambridge Street, Manchester M15 6FH

Key words: chronic, inflammation, periodontitis, cytokines, NETs, chemotaxis
Total character count: 31,573
Total table count: 3. 2 in main text, 1 supplementary table
Total figure count*:* 6
Total reference count: 67

Abbreviations

PLS - Papillon Lefévre Syndrome

CTSC – Cathepsin C

NSP – neutrophil serine proteases

IL-8/CXCL-8 – interleukin-8

fMLP - formyl-methionyl-leucyl-phenylalanine

MPO – myeloperoxidase

NE – Neutrophil elastase

CG – Cathepsin G

PR3 – Proteinase 3

MIP1α – Macrophage inhibitory protein-1 alpha

MRP - Myeloid-related proteins

Abstract

Background

Papillon-Lefévre Syndrome (PLS) is a rare inherited autosomal recessive disease, characterised by palmoplantar keratosis and severe pre-pubertal periodontitis leading to premature loss of all teeth. PLS is caused by a mutation in the cathepsin C (CTSC) gene, resulting in complete loss of activity and subsequent failure to activate immune response proteins. Periodontitis in PLS is thought to arise from failure to eliminate periodontal pathogens due to CTSC deficiency, although mechanistic pathways remain to be elucidated.

Aim

To comprehensively characterise neutrophil function in PLS.

Methods

Peripheral blood neutrophils were isolated from 5 PLS patients alongside matched healthy controls. For directional chemotactic accuracy, neutrophils were exposed to the chemoattractants macrophage inhibitory protein 1alpha (MIP1α) and formyl-Methionyl-Leucyl-Phenylalanine (fMLP) and tracked by real-time video-microscopy. Reactive Oxygen Species (ROS) generation was measured by chemiluminescence. Neutrophil Extracellular Trap (NET) formation was assayed fluorometrically and pro-inflammatory cytokine release was measured following overnight culture of neutrophils with relevant stimuli.

Results and Conclusion

Neutrophil serine protease (NSP) deficiencies resulted in a reduced ability of neutrophils to chemotax efficiently and an inability to generate NETs. NET-bound proteins were also absent in PLS. PLS neutrophils released higher levels of pro-inflammatory cytokines in un-stimulated and stimulated conditions and plasma cytokines were elevated. Notably, neutrophil chemoattractants MIP1α and CXCL-8 were elevated in PLS neutrophils as was ROS formation. We propose that relentless recruitment and accumulation of hyper-active/reactive neutrophils (cytokines, ROS), with increased tissue transit times into periodontal tissues, alongside a reduced antimicrobial capacity, creates a locally destructive chronic inflammatory cycle in PLS.

(250 words)

Introduction

Papillon-Lefèvre syndrome (PLS) is a rare inherited autosomal recessive disease characterised by diffuse palmoplantar keratosis and a severe pre-pubertal periodontitis, leading to an edentulous state in adolescence (1). Chronic periodontitis is a disorder initiated by dysbiosis within the oral plaque biofilm and which progresses due to an abnormal host inflammatory-immune response, characterised by exaggerated and non-resolving chronic inflammation, and which leads to periodontal tissue damage and bone loss (2). PLS has an estimated prevalence of 1-4 cases per million with signs and symptoms appearing between 1 and 4 years of age, typically resulting in permanent tooth loss during adolescence. There is no predominant racial or sexual predilection, however a third of reported cases involve parental consanguinity (3). Importantly, systemic immunodeficiency in PLS is relatively mild with 15-20% being pre-disposed to recurrent infections (4), yet the local periodontitis is profoundly aggressive.

PLS is caused by mutations in the gene encoding the lysosomal cysteine protease cathepsin C (CTSC), (*CTSC* gene); over 50 mutations in the gene have been reported as responsible for PLS, with phenotypes ranging from specific loss of function (resulting in a deficiency) to complete absence of the enzyme. CTSC is expressed in high levels in neutrophils and is responsible for the activation of neutrophil serine proteases (NSPs). The loss of CTSC activity causes the subsequent cessation of NSP activity (5,6). Failure of NSPs to eliminate periodontal bacteria is thought to be the underlying cause of the severe periodontal disease in PLS patients, however comprehensive and systematic characterisation of neutrophil function in PLS has been hampered by the rarity of the disease, and case studies limited to individual patients.

Neutrophils represent the first line of defence against microbial pathogens. Neutrophils resolutely survey tissues for microorganisms, and during tissue infections they extravasate the circulation into the tissues where they undergo directional movement towards the source of infection via chemical gradients (chemotaxis). This highly regulated recruitment process is orchestrated by the release of chemoattractants which may be host-derived, such as interleukin-8 (IL-8/CXCL-8) and macrophage

inflammatory protein alpha (MIP-1α), or pathogen-derived, (e.g. N-formyl-methionyl-leucyl-phenylalanine; fMLP). Neutrophils function by eradicating pathogens via phagocytosis and subsequent intracellular and extracellular killing mechanisms *in-situ*, as a vital part of innate and acquired immunity.

Phagocytosis involves pathogen internalisation and destruction via reactive oxygen species (ROS) generation following the assembly of nicotinamide adenine dinucleotide phosphate (NADPH)-oxidase at the phagosome membrane, the fusion of 4 distinct types of neutrophil granules (azurophilic/primary, specific/secondary, gelatinase/tertiary and secretory) and release of antimicrobial peptides (AMPs) into the phagosome. The azurophilic granules contain several microbicidal agents including myeloperoxidase (MPO), defensins, and various NSPs which include neutrophil elastase (NE), cathepsin G (CG), proteinase 3 (PR3) (5) and the recently described neutrophil serine protease 4 (NSP4) (7).

NSPs can be released extracellularly following limited granule exocytosis (8), binding to the external cell surface, where they target a variety of host chemokines, cytokines, growth factors and cell surface receptors contributing to both pro- and anti-inflammatory processes. PR3 has been shown to cleave active IL-8, increasing its potency (9), and to splice the inactive membrane bound pro-form of tumour necrosis factor alpha (TNFα) (10) resulting in activation. Conversely, NSP processing affects the activity of chemokines such as MIP1α (11) and IL-8 (12) resulting in their inactivation. In addition NSPs have been shown to inactivate IL-6 at inflammatory sites (13), thus NSPs appear to play a key role in orchestrating immunostimulatory signals.

One recently described neutrophil-mediated anti-microbial strategy involves the production of neutrophil extracellular traps (NETs), which comprise decondensed nuclear chromatin associated with granule-derived antimicrobial proteins including NSPs (14). The proposed role of NETs is to facilitate neutrophil containment and destruction of pathogenic organisms and though the mechanisms that lead to NET formation are not completely understood. NE and ROS have been shown to be fundamental to

NET release (15). In addition, the Specific Granule-derived AMP cathelicidin (hCAP18/LL-37) is cleaved by PR3, forming LL-37, which is also known to facilitate NET formation (16).

For decades the consensus has been that PLS patients suffer a severe pre-pubertal periodontitis as a result of NSP deficiencies failing to eliminate causative pathogens, in particular *Aggregatibacter actinomycetemcomtans* (*A. actino*) (17). However, such proposed mechanisms fail to explain the severe periodontal inflammation and associated alveolar bone destruction and subsequent tooth loss that characterises PLS-periodontitis. This relates in part to a lack of systematic evaluation of different aspects of neutrophil function, which, given the diverse range of NSP-dependent processes that in-turn require CTSC activity, are likely to reveal a more complex series of linked events that culminate in the destructive localised chronic periodontal inflammation that characterises PLS. Moreover, in the last decade it has become clear that neutrophils are not merely short-lived destructor cells, armed with a pre-packaged cytotoxic arsenal, but in fact survive for 5.4 days in the circulation (18) and are capable of more subtle synthetic activities, elaborating various signalling molecules, including pro-inflammatory cytokines (19) and myeloid-related proteins (MRPs); of note are the calcium-binding proteins S100A8 and S100A9 which represent ~45% of proteins within the neutrophil cytosol (20). S100s, also known as calgranulins, are involved in many pro-inflammatory immune processes including phagocyte migration, chemotaxis and antimicrobial defence.

Aims

In this study we aimed to comprehensively characterise peripheral blood neutrophil function from a group of PLS patients (aged between 9 and 14 years) for the first time using novel assays of directional chemotactic accuracy, neutrophil extracellular trap (NET) formation, reactive oxygen species (ROS) and cytokine release, in order to explain the likely mechanisms underpinning the local severe periodontal inflammation, in the absence of significant systemic immune dysfunction in PLS.

Methods

Blood collection and neutrophil isolation

Whole blood (up to 18ml) was collected from five adolescents from 5 different families with PLS at Birmingham Children's Hospital and five gender-matched controls. Exclusion criteria included smoking and pregnancy. Ethical approval was provided by the West Midlands/The Black Country NRES Committee (14/WM/1175).

Gender-matched young healthy controls (aged 19-21) were recruited from students within the University of Birmingham Dental School. Neutrophils were isolated by Percoll density centrifugation using two discontinuous gradients, 1.079 and 1.098, followed by erythrocyte lysis (0.83% NH_4Cl containing 1% $KHCO_3$, 0.04% EDTA and 0.25% BSA) as previously described (21). Cells were re-suspended in PBS supplemented with glucose (1mM) (gPBS) and cations (1 mM $MgCl_2$, 1.5 mM $CaCl_2$). The cells were diluted accordingly. Cell viability was determined by Trypan Blue dye exclusion (typically >98%) and cell purity by cytospin. Plasma was also prepared by centrifugation and stored at -80°C prior to further use. For all subsequent assays plasma was used neat/diluted according to relevant assay manufacturer's instructions. Due to low neutrophil counts, it was not possible for all 5 patient samples to be employed in all assays; the numbers included are specified accordingly.

NET assays

NET-DNA was quantified as previously described by our group (22). Briefly, neutrophils were resuspended in RPMI-1640 and added to a pre-blocked 96-well microplate (1×10^5 in 150µl per well). After a 30 minute baseline incubation period (37°C), selected wells were stimulated with PMA (50nM), HOCl (0.75nM) or periodontally relevant bacterial stimuli (opsonised *S. aureus*, *A. actinomycetemcomitans; A. actino,* serotype b and *Fusobacterium nucleatum*; *F. nucleatum*) at an MOI of 1000:1 to ensure NET stimulation by the bacteria. NET DNA was digested after 4 hours of incubation by the addition of micrococcal nuclease (15µl at 1 unit/ml) for 20 minutes to digest extracellular DNA after which the cells were pelleted at 1,200 RCF for 10 minutes. Supernatant (150µl) was collected into a black microplate and Sytox green (Life Technologies; 15µl, 10µM) was added. Fluorescence was read in arbitrary fluorescence units (AFU) using a fluorometer (Twinkle

LB970, Berthold Technologies). NETs were also visualised after 4 hours incubation with an epi-fluorescence microscope (Nikon Eclipse TE300).

NET-bound components were assayed within neutrophil supernatants using 96 well microplates: 1) NE - equal volumes (100µl) of supernatants and 0.5M N-MethoxysuCTSCinyl-Ala-Ala-Pro-Val p-nitroanilide were mixed; after 2 hours incubation (37°C) absorbance was measured at 405nm; 2) NET-bound MPO - equal volumes (50µl) of supernatant and 3,3',5,5'-Tetramethylbenzidine (TMB) substrate solution were mixed and incubated (20 minutes at room temperature), subsequently the reaction was stopped by addition of sodium phosphate (50µl, 1M), absorbance was measured at 540nm; 3) NET-bound CG - equal volumes (50µl) of supernatant and N-Succinyl-Ala-Ala-Pro-Phe p-nitroanilide were mixed and incubated (2 hours, 37°C) after which absorbance was measured at 405nm.

Enhanced chemiluminescence assay of ROS production

ROS were variously analysed using the chemiluminescent reagents luminol, isoluminol and lucigenin to detect total, intracellular and superoxide production respectively as previously described (19,22). Briefly, a white 96-well microplate was pre-blocked by addition of PBS with 1% BSA (200µl per well) and incubated overnight at 4°C; prior to use the liquid was aspirated off. Neutrophils were suspended in gPBS and seeded into the pre-blocked 96 well microplate (1 x 10^5 in 100µl per well). Chemilumiescent reagents were added to the appropriate wells: luminol (30µl, 3mmol/l); lucigenin (30µl, 3mmol/l); or isoluminol (60µl, 3mmol/l) with horseradish peroxidase (15µl, 6U). After a 30 minute baseline incubation period, selected wells were stimulated with PMA (25nM) to directly activate protein kinase-C (PKC) without cell surface receptor ligation or bacterial stimuli (opsonised *S. aureus* and heat-killed *A. actino*). All assays were performed at 37°C using a Berthold microplate-luminometer (LB96v).

Chemotaxis assay

The Insall chamber was employed for a novel directional chemotaxis assay (23). Neutrophils at 1 x 10^6/ml were suspended in RPMI, 400µl was added to 7.5% BSA-coated acid washed (0.2M HCl) coverslips (22mm) and incubated at room temperature for 20 minutes. The coverslip was then inverted onto the Insall chamber and excess fluid was aspirated off. Chemoattractants fMLP (10nM) and MIP1α (100ng/ml) were used along with RPMI (control). For chemotaxis with MIP1α a prior incubation step was included: granulocyte macrophage colony-stimulating factor (GM-CSF) at 200pg/ml for 30 minutes, as is required for MIP1α receptor up-regulation and effective chemotaxis (24). Each chemoattractant/buffer was injected into the chemoattractant channels and visualised using a Zeiss Primovert microscope (Carl Zeiss Imaging, Thornwood, NY, USA) and Images captured every 30 seconds for up to 40 frames per condition using a Q Imaging Retiga 2000R camera (Qimaging, Surry, Canada). The frames were processed using Q pro-imaging software (Surrey, Canada) and analysed further using ImageJ 1.45SR software (National Institutes of Health, Bethesda, USA) utilising the manual tracking MtrackJ plug-in. For each condition 15 cells were tracked and the data generated was used to calculate speed, velocity and chemotactic index as previously described (25–27).

Cell culture

Neutrophils were cultured overnight as previously described (19,28). Briefly, isolated neutrophils (at 2.5 x 10^6/ml) were suspended in RPMI-1640 supplemented with 0.3 g/l glutamine, 0.232 g/l HEPES, 100 mg/ml streptomycin and 10% low endotoxin fetal calf serum. Cultures were incubated for 18 hours at 37°C and 5% CO_2 with and without bacterial stimuli as used to measure both NETs and ROS (MOI 1 in 100), after which the supernatants were collected and stored at -80°C until further analysis of strategically relevant cytokines, MMP9, NE, LL37 and S100A-8/9.

Multiplex assay of neutrophil cytokine and MMP-9 Release

Pro-inflammatory cytokine (IL-1β, IL-6, IL-8, MIP1α, TNFα) and matrix metalloproteinase-9 (MMP-9) release were measured using Procartaplex™ multiplex immunoassays (Affymetrix-eBioscence) according to the manufacturer's instructions.

Enzyme linked immunosorbent assay (ELISA) of AMPs

Neutrophil elastase (NE), LL-37 and S100A-8/9 were quantified from neutrophil cell cultures and plasma samples via ELISA assays (eBiosciences, Hycult Biotech and R & D Systems respectively) according to the manufacturer's instructions.

Plasma protein oxidation

In addition plasma protein carbonylation was assayed as a measure of oxidative damage, as previously described (29). Briefly, the protein content of the plasma samples was measured using bicinchoninic acid (BCA) assay. Oxidised standards (prepared using sodium borohydride) and plasma samples were diluted in carbonate buffer (pH 9.6, 0.05 M) to 20mg/ml and 50µl of each was pipetted in triplicate into a Nunc-Immuno plate, Maxisorp. Samples were derivatised directly on the plate using 1mM DNPH in 2M HCl. Following three washes, the plate was incubated with blocking buffer (Tween 20 (1% v/v) in PBS), overnight at 4°C. After incubating for 2 h at 37 °C with monoclonal mouse anti-DNP (Sigma, UK) antibody diluted 1:2000 in 1% BSA, the bound antibody was detected with peroxidase-conjugated rat anti-mouse IgE antibody (AbD Serotec, diluted 1:5000 in blocking buffer), 50µl citrate phosphate buffer pH 5.0, 0.15M, containing 20mg tablet o-phenylenediamine and 10µl 8.8M hydrogen peroxide. The reaction was terminated by addition of 25µl 2M $H_2 2SO_4$. Absorbance was measured spectrophotometrically at 490nm, using a BioTek plate reader (BioTek, UK). Carbonyl content was calculated from the standard curve and expressed as nanomol carbonyls per milligram of protein.

Statistical analysis

Statistical analyses included (where levels were detectable): NETs, ROS, luminex and ELISA assays using Mann-Whitney and Kruskal-Wallis test. Chemotaxis was analysed by Mann Whitney test.

Results

Table 1 provides summary patient demographics and CTCG mutation analyses.

Quantification of NE and LL-37 from neutrophil culture supernatants and patient plasma

NE and LL-37 were quantified in plasma and also from cultured neutrophil supernatants both unstimulated and following TLR- and FcγR-stimulation (**Figure 1a-d**) and from plasma. Both proteins are activated by CTSC; NE is activated by CTSC directly and LL-37 is activated via PR3 (30), following PR3 activation by CTSC. NE was almost completely absent in both plamsa and neutrophil supernatants. LL-37 was absent in plasma from PLS patients but was present at low concentrations in supernatants following stimulation with heat-killed bacteria or particularly with opsonised *S. aureus*, suggesting minimal CTSC activity. These results indicate systemic and local NSP deficiency in PLS patients.

Quantification of NETs and NET bound components

The ability of PLS patients to produce NETs was determined by fluorometric quantification of NET DNA and also by colourimetric quantification of the NET-associated proteins; NE, MPO and CG. NETs and NET bound proteases were substantially decreased or deficient in patients and significantly lower (where calculated) compared to controls for all receptor stimulations evaluated (**Figure 2a-d**).

The absence of, or marked reduction in, NETs produced was confirmed by epi-fluorescence microscopy (**Figure 2e**) providing additional data to that recently reported in a single PLS patient (31). The reduced presence of NET-bound MPO further supports the lack of NET structrues in these patients, who do not otherwise suffer a MPO deficiency. NE and CG, which are both activated by cathepsin C, were also extremely low in PLS patients.

Neutrophil ROS generation and plasma protein oxidation in PLS

Total and intracellular ROS and superoxide were detected using different chemiluminescent reagents luminol, isoluminol and lucigenin respectively (**Figure 3a-c**). In all conditions ROS generation was the same or higher in PLS patients compared to controls; statistical significance was reached with the use of PMA. Protein carbonylation, a ROS-induced marker of oxidative stress was also measured in plasma to provide evidence of ROS-hyper-responsivity *ex vivo* (**Figure 3d**). These results add to

previous work demonstrating decreased antioxidant defences/increased oxidative stress (lipid hydroperoxide levels) in unstimulated neutrophils from PLS patients (32).

Cytokine, MMP-9 and S100A8/9 levels in plasma and neutrophil culture supernatants

The pro-inflammatory cytokines IL-1β, IL-6, IL-8, MIP1α and TNFα were quantified from culture supernatants and plasma samples by multiplex assay. In addition, MMP-9, the major enzyme released by neutrophils involved in the breakdown of the extracellular matrix to facilitate movement through the tissues, and the MRPs S100A8 and A9 were quantified by ELISA. **Figure 4a-h** (**Supplementary Table 1)** shows neutrophil culture supernatant levels and **Table 2** shows plasma concentrations. Within cultured neutrophil supernatants there was a significant increase in IL-6, IL-8 and MIP1α (p <0. 0286) in the absence of stimulation indicating a hyperactive neutrophil phenotype. Following TLR stimulation, cytokines IL-6, IL-8, MIP1α and TNFα were all higher in PLS than controls (p =0. 0286). In addition, S100A9 was also found to be elevated. The same results were achieved with FCγR stimulation with the exception of IL-6. The neutrophil supernatant results demonstrate that PLS neutrophils exhibit a hyper-reactive neutrophil phenotype. IL-8 and MMP9 levels were higher in PLS plasma than controls, consistent with neutrophil cell culture supernatant data.

Neutrophil chemotaxis in PLS

Neutrophil directional chemotactic accuracy was measured in PLS using the Insall chamber. Speed (overall cell movement), velocity (movement in the direction of the chemoattractant source) and chemotactic index (a measure of the accuracy of cell orientation) were measured over time in the presence of buffer or chemoattractant. Speed was significantly lower in patients when exposed to MIP1α (**Figure 5a**), a trend that was consistent for both MIP1α & fMLP when velocity (**5b**) and chemotactic index (**5c**) were measured. **Figure 5d** shows the cell paths of all tracked cells per condition, illustrating the differences in the course of the cell movements. MIP1α is a target for NSPs which deactivate MIP-1α. As NSP function is lost in PLS individuals, MIP1α was employed in the chemotaxis assays to ascertain whether neutrophils from PLS patients chemotax differently to those from healthy controls and whether MIP1α chemotaxis is at all enhanced in PLS patients over controls.

PLS patient neutrophils showed significantly reduced speed, velocity and chemotactic accuracy compared with controls in response to MIP1α, and also a lower chemotactic index (accuracy of movement) in response to fMLP.

Discussion

This is, to our knowledge the most comprehensive analysis of neutrophil function in PLS patients compared with unaffected controls and the first to explore directional chemotaxis and cytokine release as part of the neutrophil repetoire. PLS neutrophils demonstrated negligible NET formation as analysed by assays of NET DNA and an almost total absence of the NET-associated AMPs - CG, NE and MPO, despite the fact that PLS neutrophils are not MPO deficient as previously reported (33). NE and CG are both enzymes that are activated by CTSC, and *in vitro* studies of NSPs have demonstrated CG and NE are able to kill *A. actinomycetemcomitans* in addition to other periodotal bacteria (34), and so their deficiency likely compromises neutrophil antimicrobial efficacy allowing for the persistance of some pathogenic species over others in PLS. NE is necessary for NETosis as demonstrated by the study of neutrophil elastase disorders such as *ELA2*-related neutropenia, where neutrophil elastase activity is deficient (35) and NET formation is diminished. Conversely in *HAX1*-related neutropenia elastase is functional and *HAX1*-neutropenia patients produce NETs (36).

The ROS data indicate an enhanced response to PMA in PLS, consistent with a hyper-reactive neutrophil phenotype (21) which may contribute significantly to the oxidative stress (elevated lipid hydroperoxide levels) and antioxidant compromise previously reported in PLS (22). The increased ROS detected in PLS patient neutrophils may contribute to host-mediated periodontal tissue damage at sites where neutrophils are the dominant immune cell, such as the periodontium.

Cytokine measurements demonstrated neutrophil hyper-activity in PLS, with increased release of pro-inflammatory cytokines (IL-6, IL-8 and MIP1α) from unstimulated cells. This was further supported by elevated cytokine levels in patient's plasma relative to controls. In addition, MMP9 levels were also elevated in PLS patient plasma. Furthermore hyper-reactivity (to a stimulus) in terms of pro-

inflammatory cytokine release and also S100A9 concentration was also evident from the supernatants of stimulated cultured neutrophils. Higher S100A8/9 concentrations have been reported in inflamed tissues and are known to be markers of neutrophil activation (37). Interestingly S100A9 is a target for CG (38) to generate neutrophil immobilising factor (NIF) which has been shown to inhibit neutrophil migration and chemotaxis *in vitro* (39). The action of NIF may represent one means of limiting the neutrophil influx into inflammatory lesions, and its absence may contribute to the non-resolving, destructive local inflammation evident in PLS. Conversely, higher levels of S100A9 in PLS, which can form a heterodimer with S100A8 has been shown to be involved in the assembly of the NADPH oxidase complex (40), which may explain the heightened ROS levels in our PLS studies.

Neutrophil chemotaxis was shown to be defective in PLS patients, potentially increasing neutrophil tissue transit times and further potentiating neutrophil-mediated tissue damage. NSPs de-activate MIP1α and IL-8 and the loss of NSP function in PLS may result in relentless neutrophil recruitment to periodontal tissues by such chemokines. Neutrophil speed and velocity were also reduced in response to MIP1α, relative to controls, and there was a significant difference in directional chemotactic accuracy of PLS neutrophils for both MIP1α and fMLP. Previous studies that identified impaired chemotaxis in PLS were performed using different assays to those presented in this study; such as the Boyden chamber (41), and the Zymosan activated serum (ZAS) assay (42). The latter assays do not measure directional chemotaxis, unlike the direct visualisation chamber employed in our study. Indeed real-time observation of migrating cells by time-lapse video microscopy is considered the "gold standard" for investigating chemotaxis (43).

Taken together the data generated in this study point to two key scenarios as mechanistic explanations for PLS-periodontitis which will be discussed in turn: a) relentless recruitment of neutrophils into periodontal tissues where tissue transit times are increased and b) compromised anti-microbial killing.

a) **Relentless recruitment of hyper-active/reactive neutrophils into periodontal tissues**

The importance of NSPs in the antimicrobial functionality of neutrophils, and the implications of NSP deficiency for the development of periodontitis, have been previously reported (4,17). In addition

neutrophils lacking both NE and CG were unable to undergo cytoskeletal reorganisation despite adhering to immune-complex-coated surfaces *in vitro* (41), the underlying cause being a decrease in the phosphorylation of the GTPase RAC1 which is performed indirectly by CG; the lack of NSPs in PLS may therefore be an underlying cause of the chemotactic defect reported here. Moreover, MIP-1α isoforms are inactivated by NSPs (11), and MIP-1α has been shown to act as an osteoclast activation factor, inducing bone resorption (45). Thus we propose that the constant presence of active MIP1α and failure to generate NIF (not reported here) in PLS may drive a relentless recruitment and accumulation of activated neutrophils to the inflamed periodontal tissues and lead to the subsequent destruction of periodontal connective tissue and alveolar bone evident in PLS patients. Such a homeostatic imbalance would not manifest systemically due to the absence of a constant microbial challenge, such as is present in the periodontal tissues. In addition, the deficiency of LL-37, itself a result of PR3 deficiency in PLS patients, increases the incidence of microbial infection, notably with the periodontal pathogen *A. actinomycetemcomitans* (33). NSP dysfunction is associated with periodontal disease in other syndromes, including Chediak Higashi Syndrome (46) and the allelic variant to PLS, Haim Munk Syndrome (47). Furthermore, neutrophils from sufferers of Specific Granule Deficiency, characterised by defects in the packaging of azurophil and specific granules (which contain NSPs and NADPH oxidase components respectively), have been shown to exhibit decreased phagocytosis, diminished ROS formation and reduced chemotaxis (48).

b) **Compromised antimicrobial killing**

PLS patients suffer modest systemic infections, with 15-20% patients reporting recurrent infections, unlike patients with chronic granulomatous disease (CGD) charactersied by the lack of a functional NADPH oxidase and the subsequent inability to produce ROS or form NETs. Interestingly CGD patients are not overtly susceptible to periodontitis (49), suggesting that the periodontal tissue destruction seen in PLS cannot be fully explained by compromised neutrophil anti-microbial defences. PLS individuals are not systemically immunocompromised and our reported results demonstrate PLS neutrophils have the capacity to respond to pathogenic stimuli, thus NSPs do not constitute the primary antimicrobial defence mechanism, and the underlying cause of periodontitis in

PLS cannot be explained by reduced neutrophil bacterial killing alone. We propose that the periodontal tissue damage in PLS patient's results from a complex series of events arising downstream of the CTSC deficiency and dependent upon a diverse range of NSP functions that are normally active at sites of microbial challenge. Specifically, impaired bacterial killing, results in persistence of pathogenic species and triggers the relentless recruitment of hyper-active and reactive neutrophils in terms of ROS and pro-inflammatory cytokines into the periodontium. The latter, augmented by extended tissue transit times and a failure to de-activate MIP1α, likely drives the connective tissue damage and bone loss in PLS. Defects in neutrophil function have been shown in several studies of chronic periodontitis patients; peripheral neutrophils from chronic periodontitis patients exhibit hyper-reactivity with respect to ROS release (21) and pro-inflammatory cytokine production (19) in response to a microbial challenge, and also hyperactivity in the absence of an exogenous stimulant (50). Chemotaxis in chronic periodontitis patients has also been found to be defective with only partial improvement after non-surgical therapy (27), and oxidative stress is also a strong feature of periodontitis. In PLS, failure to activate and release NSPs appears to exaggerate the above defects and offers a more plausible explanation for the aggressive periodontal tissue damage seen in PLS than one based purely on defective anti-microbial defences.

Conclusion

This study has characterised, for the first time, a range of neutrophil behaviours in PLS patients from 5 different families and provided new insights into the functional consequences of Cathepsin C deficiency upon periodontal tissue destruction and tooth loss. Our results show that PLS neutrophils have a substantially reduced capacity for NET production, with NET visualisation data confirmed by the almost total absence of NET-related proteins CG, NE and MPO. ROS generation was higher in PLS and chemotactic speed and velocity to a MIP-1α stimulus was reduced, with defective directional chemotactic accuracy towards both fMLP and MIP-1α. Thus we have demonstrated a range of functional neutrophil defects in PLS, arising secondary to the CTSC deficiency and consequent failure to activate NSPs, the cumulative effects of which may conspire to destroy periodontal tissues. The failure of key neutrophil antimicrobial activities, likely maintains a stimulus for a misdirected

recruitment of hyper-responsive neutrophils into periodontal tissues, and provides a plausible explanation for the severe inflammation and bone loss that characterises PLS-periodontitis. Interestingly, PLS individuals do not suffer systemic infections, other than rarely reported skin abscesses, therefore the neutrophil defects appear specifically localised to areas of the body susceptible to a direct and chronic bacterial challenge.

Acknowledgements

This work was supported by the Black Country Comprehensive Local Research Network (NIHR UKCRN) Study ID 14/WM/1175, and the Medical research Council grant number MR/J500434/1. The authors wish to acknowledge Francesca Liu for her assistance with the Luminex assays, Michael Dudley for his support setting up the clinical study and Dr Thomas Hart for initial discussions about MIP-1α.

Conflict of interest disclosure

The authors have no conflict of interest to disclose.

References

1. Dhanrajani, P.J. (2009) Papillon-Lefèvre syndrome: clinical presentation and a brief review. *Oral Surg. Oral Med. Oral Pathol. Oral Radiol. Endod.* **108**, e1–7.

2. Meyle, J. and Chapple I. (2015) Molecular aspects of the pathogenesis of periodontitis. *Periodontol. 2000.* **69**, 7–17.

3. Hart, T.C., Shapira, L. (1994) Papillon-Lefèvre syndrome. *Periodontol. 2000.* **6**, 88–100.

4. Pham, C.T.N., Ivanovich, J.L., Raptis, S.Z., Zehnbauer, B., Ley, T.J. (2004) Papillon-Lefèvre syndrome: correlating the molecular, cellular, and clinical consequences of cathepsin C/dipeptidyl peptidase I deficiency in humans. *J. Immunol.* **173**, 7277–81.

5. De Haar, S.F., Jansen, D.C., Schoenmaker, T., De Vree, H., Everts, V., Beertsen, W. (2004) Loss-of-function mutations in cathepsin C in two families with Papillon-Lefèvre Syndrome are associated with deficiency of serine proteinases in PMNs. *Hum. Mutat.* **23**, 524.

6. Pham, C.T., Ley, T.J. (1999) Dipeptidyl peptidase I is required for the processing and activation of granzymes A and B in vivo. *Proc. Natl. Acad. Sci. USA* **96**, 8627–32.

7. Perera, N.C., Schilling, O., Kittel, H., Back, W., Kremmer, E., Jenne, D.E. (2012) NSP4, an elastase-related protease in human neutrophils with arginine specificity. *Proc. Natl. Acad. Sci. USA* **109**, 6229–34.

8. Owen, C.A., Campbell, E.J. The cell biology of leukocyte-mediated proteolysis. (1999). *J. Leukoc. Biol*. **65**,137–50.

9. Padrines, M., Wolf, M., Walz, A., Baggiolini, M. (1994) Interleukin-8 processing by neutrophil elastase, cathepsin G and proteinase-3. *FEBS Lett*. **352**, 231–5.

10. Armstrong, L., Godinho, S.I.H., Uppington, K.M., Whittington, H.A., Millar, A.B. (2009) Tumour necrosis factor-alpha processing in interstitial lung disease: a potential role for exogenous proteinase-3. *Clin. Exp. Immunol*. **156**, 336–43.

11. Ryu, O.H., Choi, S.J., Firatli, E., Choi, S.W., Hart, P.S., Shen, R-F., et al. (2005) Proteolysis of macrophage inflammatory protein-1alpha isoforms LD78β and LD78α by neutrophil-derived serine proteases. *J. Biol. Chem*. **280**, 17415–21.

12. Leavell, K., Peterson, M., Gross, T. (1997) Human neutrophil elastase abolishes interleukin-8 chemotactic activity. *J. Leukoc. Biol*. **61**, 361–6.

13. Bank, U., Küpper, B., Ansorge, S. (2000) Inactivation of interleukin-6 by neutrophil proteases at sites of inflammation. Protective effects of soluble IL-6 receptor chains. *Adv. Exp. Med. Biol*. **477**, 431–7.

14. Brinkmann, V., Reichard, U., Goosmann, C., Fauler, B., Uhlemann, Y., Weiss DS, et al. (2004) Neutrophil extracellular traps kill bacteria. *Science.* **303**, 1532–5.

15. Papayannopoulos, V., Metzler, K.D., Hakkim, A., Zychlinsky, A. (2010) Neutrophil elastase and myeloperoxidase regulate the formation of neutrophil extracellular traps. *J. Cell Biol*. **191**, 677–91.

16. Neumann, A., Berends, E.T.M., Nerlich, A., Molhoek, E.M., Gallo, R.L., Meerloo, T., et al. (2014) The antimicrobial peptide LL-37 facilitates the formation of neutrophil extracellular traps. *Biochem. J*. **464**, 3–11.

17. De Haar, S.F., Hiemstra, P.S., van Steenbergen, M.T.J.M., Everts, V., Beertsen, W. (2006) Role of polymorphonuclear leukocyte-derived serine proteinases in defense against Actinobacillus actinomycetemcomitans. *Infect. Immun.* **74**, 5284–91.

18. Pillay, J., den Braber, I., Vrisekoop, N., Kwast, L.M., de Boer, R.J., Borghans, J. M., et al. (2010) In vivo labeling with 2H2O reveals a human neutrophil lifespan of 5.4 days. *Blood*. **116**, 625–7.

19. Ling, M.R., Chapple, I.L., Matthews, J.B. (2015) Peripheral blood neutrophil cytokine hyper-reactivity in chronic periodontitis. *Innate Immun*. **21**, 714–25.

20. Edgeworth, J., Gorman, M., Bennett, R., Freemont, P., Hogg, N. (1991) Identification of p8,14 as a highly abundant heterodimeric calcium binding protein complex of myeloid cells. *J. Biol. Chem*. **266**, 7706–13.

21. Matthews, J.B., Wright, H.J., Roberts, A., Ling-Mountford, N., Cooper, P.R., Chapple, I.L.C. (2007) Neutrophil hyper-responsiveness in periodontitis. *J. Dent. Res.* **86**, 718–22.

22. Palmer, L.J., Cooper, P.R., Ling, M.R., Wright, H.J., Huissoon, A., Chapple, I.L.C. (2012) Hypochlorous acid regulates neutrophil extracellular trap release in humans. *Clin. Exp. Immunol.* **167**, 261–8.

23. Muinonen-Martin, A.J., Veltman, D.M., Kalna, G., Insall, R.H. (2010) An improved chamber for direct visualisation of chemotaxis. *PLoS One* **5**, e15309.

24. Cheng, S.S., Lai, J.J., Lukacs, N.W., Kunkel, S.L. (2001) Granulocyte-Macrophage Colony Stimulating Factor Up-Regulates CCR1 in Human Neutrophils. *J. Immunol.* **166**, 1178–84.

25. Sapey, E., Stockley, J.A., Greenwood, H., Ahmad, A., Bayley, D., Lord, J.M., et al. (2011) Behavioral and structural differences in migrating peripheral neutrophils from patients with chronic obstructive pulmonary disease. *Am. J. Respir. Crit. Care Med.* **183**, 1176–86.

26. Muinonen-Martin, A.J., Knecht, D.A., Veltman, D.M., Thomason, P.A., Kalna, G., Insall, R.H. (2013) Measuring chemotaxis using direct visualization microscope chambers. *Methods Mol. Biol.* **1046**, 307–21.

27. Roberts, H.M., Ling, M.R., Insall, R., Kalna, G., Spengler, J., Grant, M.M., et al. (2015) Impaired neutrophil directional chemotactic accuracy in chronic periodontitis patients. *J. Clin. Periodontol.* **42**, 1–11.

28. Hatanaka, E., Monteagudo, P.T., Marrocos, M.S.M., Campa, A. (2006) Neutrophils and monocytes as potentially important sources of proinflammatory cytokines in diabetes. *Clin. Exp. Immunol.* **146**, 443–7.

29. Carty, J.L., Bevan, R., Waller, H., Mistry, N., Cooke, M., Lunec, J., et al. (2000) The effects of vitamin C supplementation on protein oxidation in healthy volunteers. *Biochem. Biophys. Res. Commun.* **273**, 729–35.

30. Sørensen, O.E., Follin, P., Johnsen, A.H., Calafat, J., Tjabringa, G.S., Hiemstra, P.S., et al. (2001) Human cathelicidin, hCAP-18, is processed to the antimicrobial peptide LL-37 by extracellular cleavage with proteinase 3. *Blood.* **97**, 3951–9.

31. Sørensen, O.E., Clemmensen, S.N., Dahl, S.L., Østergaard, O., Heegaard, N.H., Glenthøj, A., et al. (2014) Papillon-Lefèvre syndrome patient reveals species-dependent requirements for neutrophil defenses. *J. Clin. Invest.* **124**, 4539–48. 45.

32. Battino, M., Ferreiro, M.S., Bompadre, S., Leone, L., Mosca, F., Bullon, P. (2001) Elevated hydroperoxide levels and antioxidant patterns in Papillon-Lefèvre syndrome. *J. Periodontol.* **72**, 1760–6.

33. Eick, S., Puklo, M., Adamowicz, K., Kantyka, T., Hiemstra, P., Stennicke, H., et al. (2014) Lack of cathelicidin processing in Papillon-Lefèvre syndrome patients reveals essential role of LL-37 in periodontal homeostasis. *Orphanet J. Rare Dis.* **9**, 148.

34. Bangalore, N., J. Travis, V. C. Onunka, J. Pohl, and W. M. Shafer. (1990) Identification of the primary antimicrobial domains in human neutrophil cathepsin G. *J. Biol. Chem.* **265**:13584–13588.

35. Dale, D.C., Person, R.E., Bolyard, A.A., Aprikyan, A.G., Bos, C., Bonilla, M.A., et al. (2000) Mutations in the gene encoding neutrophil elastase in congenital and cyclic neutropenia. *Blood* 96, 2317–22.

36. Happle, C., Germeshausen, M., Zeidler, C., Welte, K., Skokowa J. (2011) Neutrophil Extracellular Traps (NETs) in Patients with Congenital Neutropenia. *53rd American Society of Haematology Annual Meeting, San Diego*.

37. Foell, D., Wittkowski, H., Vogl, T., Roth, J. (2007) S100 proteins expressed in phagocytes: a novel group of damage-associated molecular pattern molecules. *J. Leukoc. Biol*. **81**, 28–37.

38. Ryckman, C., Vandal, K., Rouleau, P., Talbot, M., Tessier, P.A. (2003) Proinflammatory activities of S100: proteins S100A8, S100A9, and S100A8/A9 induce neutrophil chemotaxis and adhesion. *J. Immunol*. **170**, 3233–42.

39. Goetzi, E.J., Austen, K.F. (1972) A neutrophil-immobilizing factor derived from human leukocytes : I. Generation and partial characterization. *J. Exp. Med*. **136**, 1564–80.

40. Kerkhoff, C., Nacken, W., Benedyk, M., Dagher, M.C., Sopalla, C., Doussiere, J. (2005) The arachidonic acid-binding protein S100A8/A9 promotes NADPH oxidase activation by interaction with p67phox and Rac-2. *FASEB J*. **19**, 467–9.

41. Djawari, D. (1978) Deficient Phagocytic Function in Papillon-Lefèvre Syndrome. *Dermatology*. **156**, 189–92.

42. Firatli, E., Tüzün, B., Efeoğlu, A. (1996) Papillon-Lefèvre syndrome. Analysis of neutrophil chemotaxis. *J. Periodontol*. **67**, 617–20.

43. Sackmann, E.K., Fulton, A.L., Beebe, D.J. (2014) The present and future role of microfluidics in biomedical research. *Nature*. **507**, 181–9.

44. Raptis, S.Z., Shapiro, S.D., Simmons, P.M., Cheng, A.M., Pham, C.T.N. Serine protease cathepsin G regulates adhesion-dependent neutrophil effector functions by modulating integrin clustering. *Immunity*. **22**, 679–91.

45. Choi, S.J., Cruz, J.C., Craig, F., Chung, H., Devlin, R.D., Roodman, G.D., et al. (2000) Macrophage inflammatory protein 1-alpha is a potential osteoclast stimulatory factor in multiple myeloma. *Blood*. **96**, 671–5.

46. Holt, O.J., Gallo, F., Griffiths, G.M. (2006) Regulating secretory lysosomes. *J. Biochem*. **140**, 7–12.

47. Hart, T.C., Hart, P.S., Michalec, M.D., Zhang, Y., Firatli, E., Van Dyke, T.E., et al. (2000) Haim-Munk syndrome and Papillon-Lefèvre syndrome are allelic mutations in cathepsin C. *J Med. Genet*. **37**, 88–94.

48. Gallin, J.I., Fletcher, M.P., Seligmann, B.E., Hoffstein, S., Cehrs, K., Mounessa, N. (1982) Human neutrophil-specific granule deficiency: a model to assess the role of neutrophil-specific granules in the evolution of the inflammatory response. *Blood*. **59**, 1317–29.

49. Nussbaum, G., Shapira, L. (2011) How has neutrophil research improved our understanding of periodontal pathogenesis? *J. Clin. Periodontol*. **38**, 49–59.

50. Matthews, J.B., Wright, H.J., Roberts, A., Cooper, P.R., Chapple, I.L.C. (2007) Hyperactivity and reactivity of peripheral blood neutrophils in chronic periodontitis. *Clin. Exp. Immunol.* **147**, 255–64.

Legends

Table 1. Table 1. Characteristics of patients recruited. All volunteers had severe pre-pubertal periodontitis. Mutation analysis was by direct sequencing. Patient 1 was a compound heterozygote and had the mildest clinical phenotype, but also had a very low neutrophil count at the time of venepuncture and was thus used for the NET quantification assay only. Volunteer 2 had a Y294C mutation (maternal allele) and is thus heterozygous for this mutation. The paternal allele was not detected and is probably within the intronic region that was not subject to analyses.

Table 2. Cytokine, MMP-9 and S100A8 and -9 concentrations from plasma collected from PLS patients and controls (n = 4 repsectively). n.d. = not detected.

Supplementary Table 1. Cytokine, MMP-9 and S100A8 and -9 release from patient and control neutrophils (n = 4 respectively) isolated and cultured for 16 hours and incubated with RPMI (control), *A. actinomycetemcomitans* or opsonised *S. aureus*. n.d. = not detected. Green text highlights results deemed significantly different at $p<0.05$.

Figure 1. Neutrophil elastase and LL-37 were quantified from plasma (**a** and **b** respectively) and from neutrophil culture supernatants, (**c** and **d** respectively). The bacteria used stimulate via different cell signaling pathways; opsonised *S. aureus* via FcγR and *A. actinomycetemcomitans* (*A. actino)* via Toll-like receptors (TLR). Due to undetectable concentrations in the patient samples no statistical analyses were performed. Blue hollow circles and filled red circles represent control and patient samples (n = 4) respectively.

Figure 2. NETs and NET bound proteins were quantified in response to PBS (neutral control), PMA (50nM), HOCl (0.75 mM) or bacteria (MOI 1 in 1000). These stimuli trigger NET formation in different ways; HOCl, is the down-stream ROS required for NET release, and whose exogenous addition bypasses NADPH-oxidase activation; PMA crosses the cell membrane and directly activates protein kinase C (PKC) allowing for NET release; and Toll-Like receptor (TLR) stimulation using heat-killed bacteria was also employed. Bacteria were selected for each assay on the basis of clinical relevance, in that they are implicated in PLS periodontitis (*A. actino*) and PLS-related skin abscesses (*S. aureus*). (**a**) NET quantification in stimulated/un-stimulated conditions (n = 5 patient n = 4 control); (**b**) NET-bound elastase detected after stimulation (n = 4); (**c**) NET-bound MPO levels (n = 3); (**d**) NET-bound CG, CG was undetectable in PLS neutrophils when stimulated with HOCl (n = 3). Blue hollow circles and filled red circles represent control and patient samples respectively. (**e**) Representative NET images in the absence of stimuli (PBS) and following the addition of PMA highlighting the lack of NET structures in PLS patients.

Figure 3. Peak values for ROS generation by neutrophils in the presence of PBS, PMA (25 nM), opsonised *S. aureus* and heat killed *A. actino* (MOI 1 in 100). Three different stimulation pathways were assayed: Fcγ receptor (using opsonised *S. aureus*); TLR (*F. nucleatum*); and direct receptor-independent stimulation of PKC by PMA. ROS production was meaured for (**a**) total ROS (detected by luminol) (n = 4); (**b**) extracellular ROS (isoluminol) (n = 4); and (**c**) superoxide (lucigenin) (n = 4) release. ROS release for patients was higher than controls with significance with PMA for all three chemiluminescent dyes. (**d**) Plasma protein carbonylation, a measure of oxidative stress, was measured by anti-DNP ELISA (n = 5). Blue hollow circles and filled red circles represent control and patient samples respectively.

Figure 4. Cytokines IL-1β (**a**), IL-6 (**b**). IL-8 (**c**), MIP1α (**d**), TNFα (**e**), MMP-9 (**f**), S100A8 (**g**) and S100A9 (**h**) release from patient and control neutrophils (n = 4 respectively) isolated and cultured for 16 hours and incubated with RPMI (control), *A. actino* (TLR stimulation pathway) or opsonised *S. aureus* (FcγR stimulation pathway). Blue hollow circles and filled red circles represent control and patient samples respectively.

Figure 5. Average speed (**a**), velocity (**b**) and chemotactic index (**c**) for patient (red) and control (blue) neutrophils. Definitions of the respective chemotaxis paramters: speed (overall cell movement), velocity (movement in the direction of the chemoattractant source) and chemotactic index (a measure of the accuracy of cell orientation). (**d**) Each cell track is overlayed for patient and control neutrophils in the presence of RPMI (neutral control), fMLP and MIP1α chemoattractants to give a qualitative overview of chemotaxis. Blue hollow circles and filled red circles represent control and patient samples (n = 4) respectively.

Tables

Table 1.

Patient no.	Age	Gender	Ethnicity	BMI	PLS type	Mutation
1	12	Male	Caucasian	18.93	Heterozygous	1/2 G139R; 1/2 N427T
2	14	Female	Indian	19.90	Heterozygous	1/2 Y294C; 1/2 not detected
3	14	Female	Pakistani	20.04	Homozygous	2/2 R272P
4	9	Male	Pakistani	22.83	Homozygous	2/2 R272P
5	15	Male	Pakistani	18.15	Homozygous	2/2 R272P
Control no.						
1	19	Male	Caucasian	20	N/A	N/A
2	20	Female	Caucasian	22	N/A	N/A
3	20	Female	Pakistani	24	N/A	N/A
4	21	Male	Pakistani	24	N/A	N/A
5	19	Male	Pakistani	23	N/A	N/A

Table 2.

Plasma									
Analyte	**Control (pg/ml)**				**Patient (pg/ml)**				***P* value**
	1	**2**	**3**	**4**	**2**	**3**	**4**	**5**	
IL-1β	0	0	0.41	0	7.06	0	1.78	0	-
IL-6	16.94	22.91	25.82	19.32	36.62	9.56	20.54	24	0.886
IL-8	0.92	1.09	0.76	0.79	3.41	1.11	3.32	1.16	0.029
MIP1α	0	27.28	4.3	0.65	36.02	11.18	32.44	5.35	0.114
TNFα	0	0	0	0	47.53	0	0.57	0	-
MMP-9	24.96	11.44	37.43	6.03	449.59	135.8	554.27	282.5	0.029
S100A8	0	0	0	0	2674.66	494.55	1436.54	2941.09	-
S100A9	0	0	0	0	1538.19	412.51	470.74	2001.63	-

Supplementary Table 1.

RPMI (Unstimulated neutrophil activity)									
Analyte	**Control (pg/ml)**				**Patient (pg/ml)**				***P* value**
	1	**2**	**3**	**4**	**2**	**3**	**4**	**5**	
IL-1β	4.38	1.34	0.65	7.58	4.8	49.37	18.15	33.9	0.057
IL-6	91.94	49.51	65.52	109.55	113.16	860.97	598.24	423.8	0.029
IL-8	1838.8	990.2	1310.4	2191	2263.2	17219.4	11964.8	8476	0.029
MIP1α	20.72	17.99	16.82	24.12	27.64	244.58	293.55	257.74	0.029
TNFα	0	0	0	0	0	17.06	13.25	19.43	-
MMP-9	786.31	1210.11	2906.7	6947.75	3,311.35	2,947.85	2,192.06	1,026.27	0.886
S100A8	367.16	227.32	248.69	384.09	331.53	171.21	695.85	233.55	0.886
S100A9	150.73	30.67	50.68	632.09	671.37	271.72	944.79	185.31	0.114
***A. actinomycetemcomitans* (neutrophil reactivity)**									
Analyte	**Control (pg/ml)**				**Patient (pg/ml)**				***P* value**
	1	**2**	**3**	**4**	**2**	**3**	**4**	**5**	
IL-1β	60.98	57.45	52.77	122.47	59.03	271.97	233.73	160.1	0.114
IL-6	502.87	338.42	307.13	401.41	843.56	3847.74	4669.62	2007.99	0.029
IL-8	10057.4	6768.4	6142.6	8028.2	16871.2	76954.8	93392.4	40159.8	0.029
MIP1α	252.06	301.12	228.88	252.31	855.99	1408.84	721.34	849.17	0.029
TNFα	16.71	31.35	17.39	56.85	81.78	189.43	173.33	135.79	0.029
MMP-9	1,224.29	1,939.96	2899.5	5,661.66	5,398.59	3,450.59	3,034.44	1,566.67	0.686
S100A8	481.18	260.27	224.64	466.93	466.93	278.09	320.84	264.73	1
S100A9	172.20	10.35	81.59	224.67	823.27	359.72	811.75	237.68	0.029
Opsonised *S. aureus* (neutrophil reactivity)									
Analyte	**Control (pg/ml)**				**Patient (pg/ml)**				***P* value**
	1	**2**	**3**	**4**	**2**	**3**	**4**	**5**	
IL-1β	81.99	85.88	102.26	87.63	81.05	358.62	389.46	131.65	0.343
IL-6	357.02	191.77	209.19	358.87	290.15	2033.56	2898.57	848.68	0.114
IL-8	7140.4	3835.4	4183.8	7177.4	5803	40671.2	57971.4	16973.6	0.029
MIP1α	194.92	181.81	164.4	270.99	478.93	475.06	613.38	435.67	0.029
TNFα	39.2	42.2	40.99	25.86	73.85	209.16	213.93	140.61	0.029
MMP-9	1265.44	3743	6016	4979	2491	1954	2554	4328	0.496
S100A8	392.99	712.78	955.95	702.08	956.84	524.83	470.49	524.83	0.885
S100A9	20.83	37.065	95.73	350.81	956.31	428.86	831.13	336.15	0.029

Figures

Figure 1.

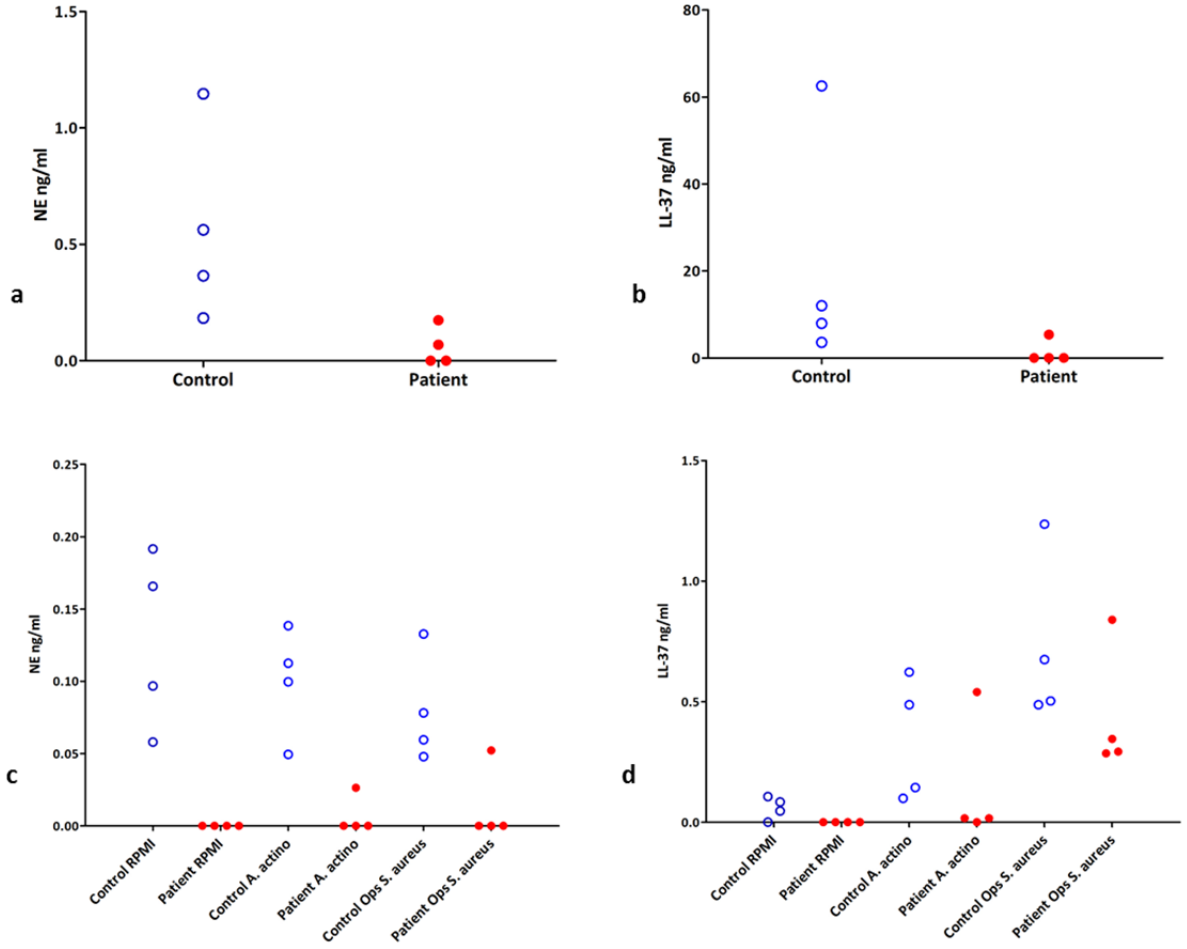

Figure 2.

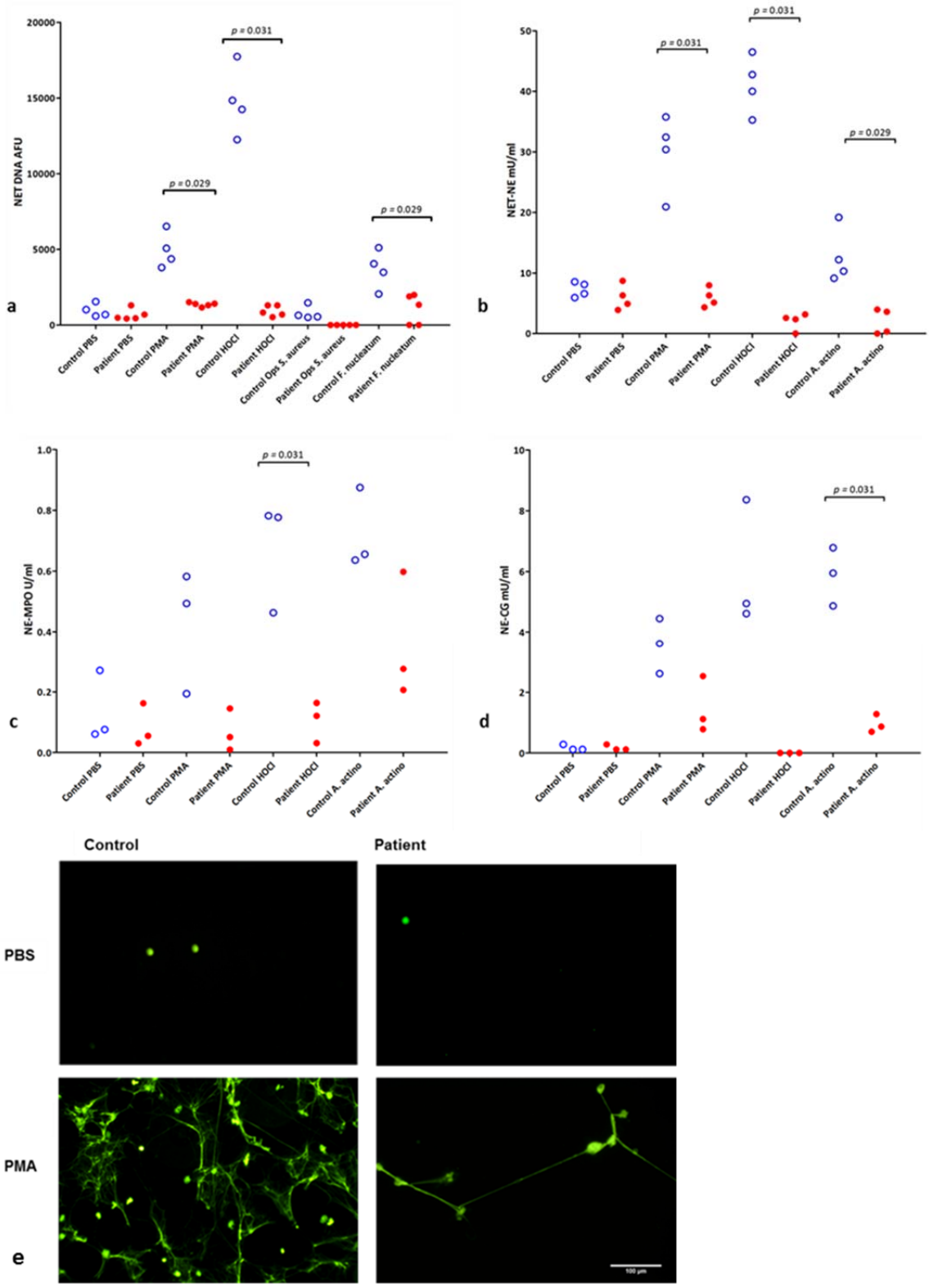
a
NET DNA AFU
20000
15000
10000
5000
0
p = 0.031
p = 0.029
p = 0.029
Control PBS
Patient PBS
Control PMA
Patient PMA
Control HOCl
Patient HOCl
Control Ops S. aureus
Patient Ops S. aureus
Control F. nucleatum
Patient F. nucleatum
b
NET-NE mU/ml
50
40
30
20
10
0
p = 0.031
p = 0.031
p = 0.029
Control PBS
Patient PBS
Control PMA
Patient PMA
Control HOCl
Patient HOCl
Control A. actino
Patient A. actino
c
NE-MPO U/ml
1.0
0.8
0.6
0.4
0.2
0.0
p = 0.031
Control PBS
Patient PBS
Control PMA
Patient PMA
Control HOCl
Patient HOCl
Control A. actino
Patient A. actino
d
NE-CG mU/ml
10
8
6
4
2
0
p = 0.031
Control PBS
Patient PBS
Control PMA
Patient PMA
Control HOCl
Patient HOCl
Control A. actino
Patient A. actino
Control
Patient
PBS
PMA
e

Figure 3.

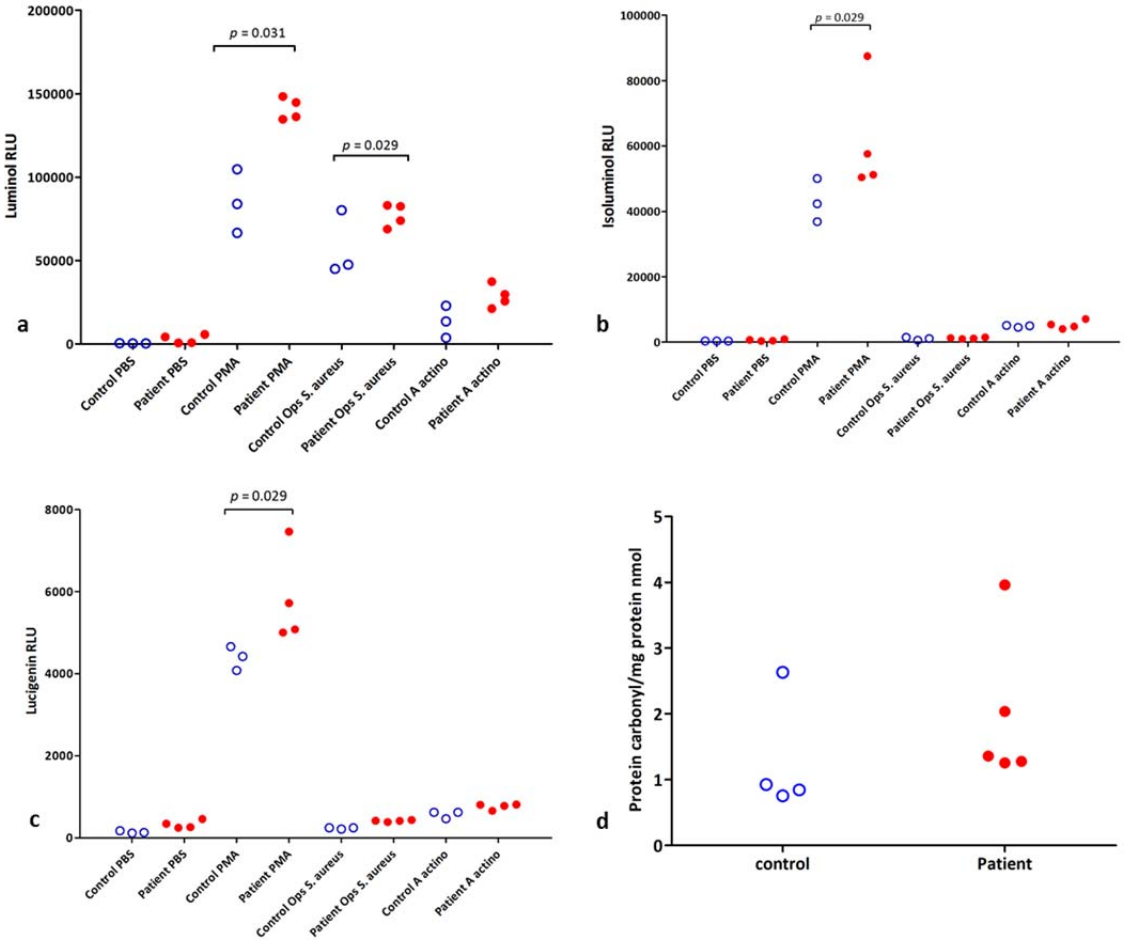
a
Luminol RLU
200000
150000
100000
50000
0
p = 0.031
p = 0.029
Control PBS
Patient PBS
Control PMA
Patient PMA
Control Ops S. aureus
Patient Ops S. aureus
Control A actino
Patient A actino
b
Isoluminol RLU
100000
80000
60000
40000
20000
0
p = 0.029
Control PBS
Patient PBS
Control PMA
Patient PMA
Control Ops S. aureus
Patient Ops S. aureus
Control A actino
Patient A actino
c
Lucigenin RLU
8000
6000
4000
2000
0
p = 0.029
Control PBS
Patient PBS
Control PMA
Patient PMA
Control Ops S. aureus
Patient Ops S. aureus
Control A actino
Patient A actino
d
Protein carbonyl/mg protein nmol
5
4
3
2
1
0
control
Patient

Figure 4

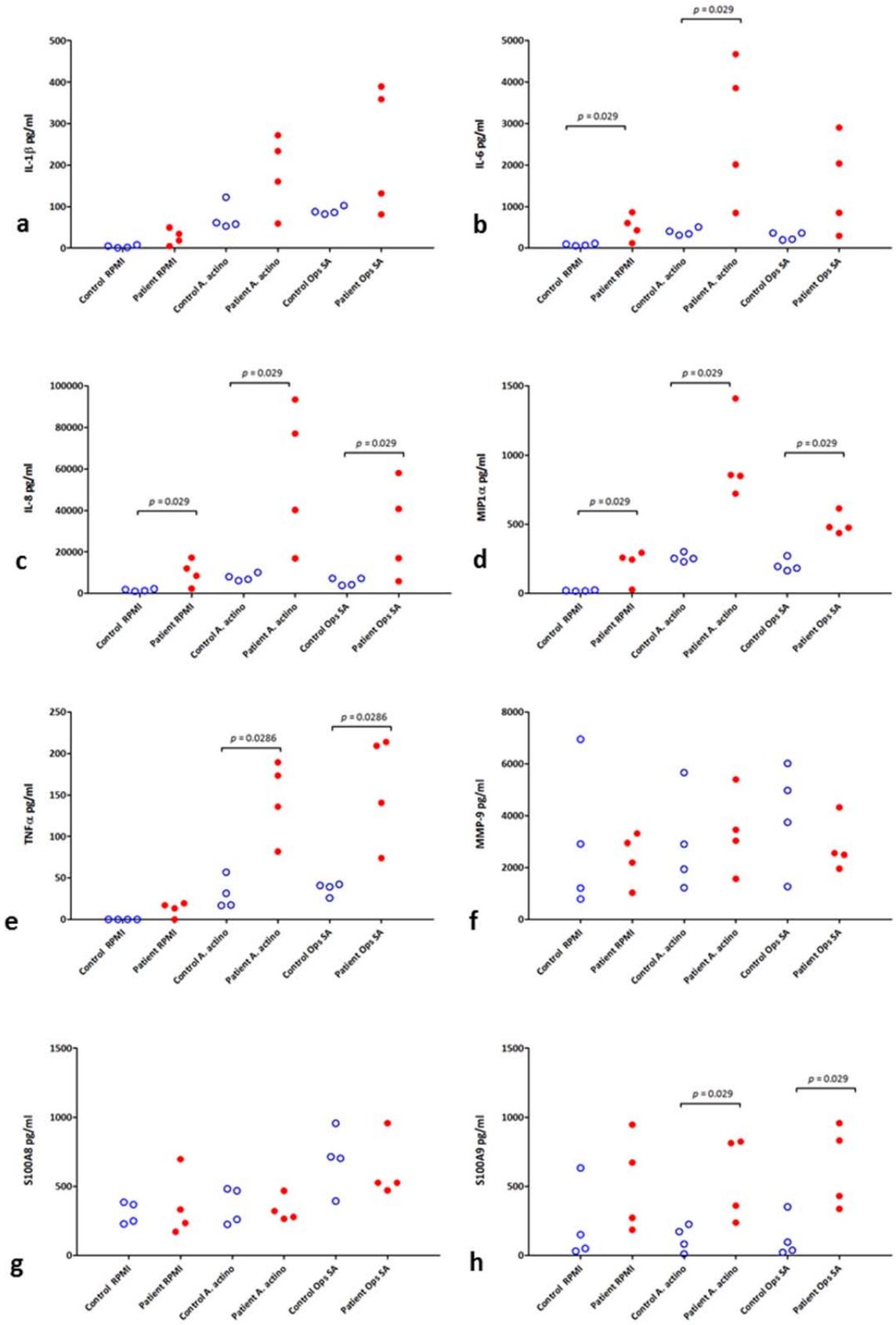
a
IL-1β pg/ml
500
400
300
200
100
0
Control RPMI
Patient RPMI
Control A. actino
Patient A. actino
Control Ops SA
Patient Ops SA
b
IL-6 pg/ml
p = 0.029
p = 0.029
5000
4000
3000
2000
1000
0
c
IL-8 pg/ml
p = 0.029
p = 0.029
p = 0.029
100000
80000
60000
40000
20000
0
d
MIP1α pg/ml
p = 0.029
p = 0.029
p = 0.029
1500
1000
500
0
e
TNFα pg/ml
p = 0.0286
p = 0.0286
250
200
150
100
50
0
f
MMP-9 pg/ml
8000
6000
4000
2000
0
g
S100A8 pg/ml
1500
1000
500
0
h
S100A9 pg/ml
p = 0.029
p = 0.029
1500
1000
500
0

Figure 5.

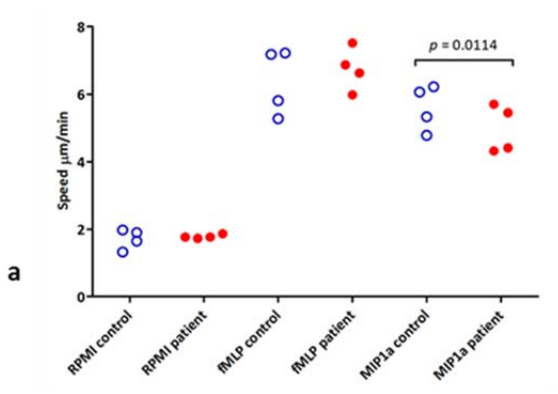
a
Speed µm/min
p = 0.0114
RPMI control
RPMI patient
fMLP control
fMLP patient
MIP1a control
MIP1a patient

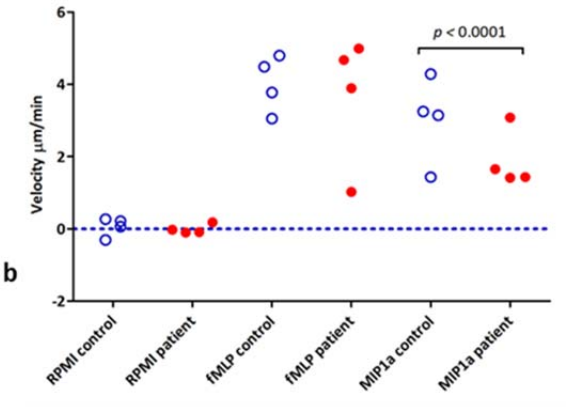
b
Velocity µm/min
p < 0.0001
RPMI control
RPMI patient
fMLP control
fMLP patient
MIP1a control
MIP1a patient

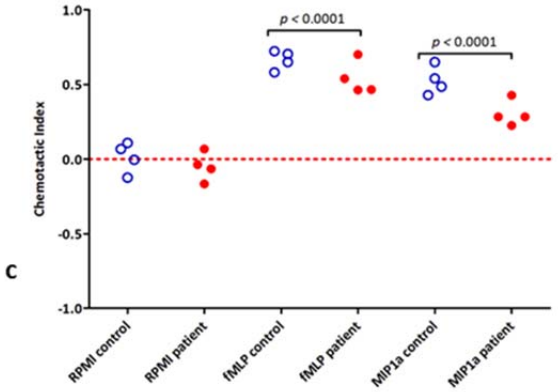
c
Chemotactic index
p < 0.0001
p < 0.0001
RPMI control
RPMI patient
fMLP control
fMLP patient
MIP1a control
MIP1a patient

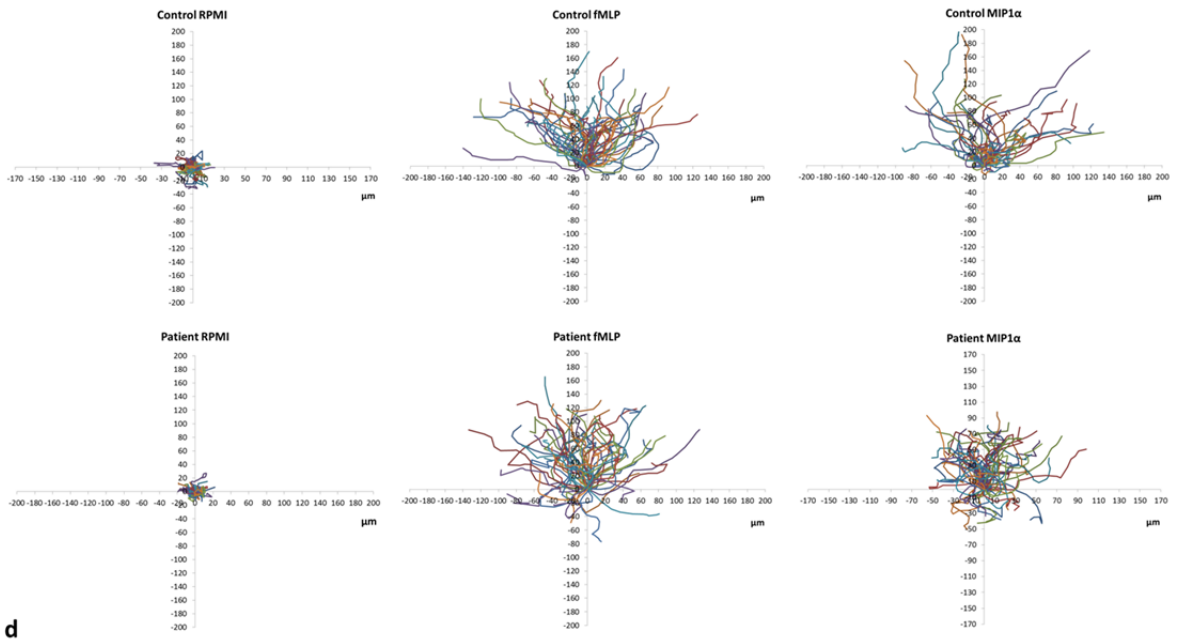
d
Control RPMI
Control fMLP
Control MIP1α
Patient RPMI
Patient fMLP
Patient MIP1α
µm